Evidence of Thermal Metamorphism on the C, G, B, and F Asteroids

Takahiro Hiroi,* Carlé M. Pieters, Michael E. Zolensky, Michael E. Lipschutz

Reflectance spectra (0.3 to 2.6 micrometers) of 14 C, G, B, and F asteroids and 21 carbonaceous chondrite powders are compared in detail. Only three thermally metamorphosed CM-CI chondrites that have a weak ultraviolet absorption are shown to have close counterparts among those asteroids. Reflectance spectra of heated Murchison CM2 chondrite are compared with the average C and G type asteroid spectra. Murchison heated at 600° to 1000°C exhibits a similar weak ultraviolet absorption and provides the best analog for those spectra. Comparison of ultraviolet absorption strengths between 160 C, G, B, and F asteroids and carbonaceous chondrites suggests that surface minerals of most of those asteroids are thermally metamorphosed at temperatures around 600° to 1000°C.

The C, G, B, and F asteroids (*1*) are distinct from other asteroids because of their low albedos and relatively featureless reflectance spectra. They have been believed to be the counterparts of carbonaceous chondrites, on the basis of their albedos and reflectance spectra in the wavelength range of 0.3 to 1.1 μm (*2*). Significant mineralogical information is also contained in longer near-infrared wavelengths up to 2.6 μm (*3*), although not many studies have been done to compare the C, G, B, and F asteroids with carbonaceous chondrites. In this report, telescopic reflectance spectra (0.3 to 2.6 μm) of the C, G, B, and F asteroids are compared with laboratory reflectance spectra of carbonaceous chondrite powders in detail.

Shown in Fig. 1 are telescopic reflectance spectra of 14 C, G, B, and F asteroids (*4*) and laboratory bidirectional reflectance spectra of 21 carbonaceous chondrite powders. These asteroids may not necessarily represent the C, G, B, and F class population but were chosen because both the 24- and 52-color reflectance data (*4*) were available for them. These asteroids and carbonaceous chondrites have almost featureless reflectance spectra except for the ultraviolet (UV) absorption edge around 0.34 μm and the weak absorption bands around 0.7 to 1.1 μm of CM2 chondrites. The main difference between the spectra of these asteroids and those of carbonaceous chondrites is the strength of the UV absorption. Most carbonaceous chondrites exhibit a stronger UV turndown than do these asteroids. Reflectances at a wavelength of 0.34 μm of the C, G, B, and F asteroids are higher than those of carbonaceous chondrites except for three unusual CI-CM chondrites—B7904, Y82162, and Y86720. These three are unusual because they have characteristics of both CI and CM groups with evidence of late-stage thermal metamorphism of differing degrees (*5*).

By comparison of the reflectance spectra of the C, G, B, and F asteroids and carbonaceous chondrites (Fig. 1), three pairs of close counterparts have been found: 1 Ceres and Y86720, 31 Euphrosyne and B7904, and 704 Interamnia and Y82162. Spectra of these asteroids and meteorites are shown in Fig. 2 (*6*). The relative brightnesses of those asteroids and of their meteorite counterparts are of the same order. The spectral shapes around 0.45 μm and the infrared astronomical satellite (IRAS) albedos (before being scaled by 0.65) of these asteroids are markedly different from those of meteorites, which suggests that other materials may also exist on those asteroids.

All of the meteorite counterparts in Fig. 2 are naturally heated CI-CM chondrites, and their counterpart asteroids include three different classes: C, G, and F. The other common carbonaceous chondrites are CI, CM, CR, CV, and CK, which differ slightly petrologically and in bulk composition. They do not have close counterparts among the 14 tested C, G, B, and F asteroids because the UV absorption strengths of common carbonaceous chondrites are much stronger than those of the C, G, B, and F asteroids.

The naturally heated CI-CM chondrites that are spectrally similar to the C, G, B, and F asteroids show petrologic evidence of thermal metamorphism (*5*). Therefore, the asteroid data were compared with material produced by heating experiments (*7*) of Murchison (CM2, the most common type of carbonaceous chondrite) to simulate metamorphism. Bulk samples of Murchison were heated in low-pressure (initially 10^{-5}

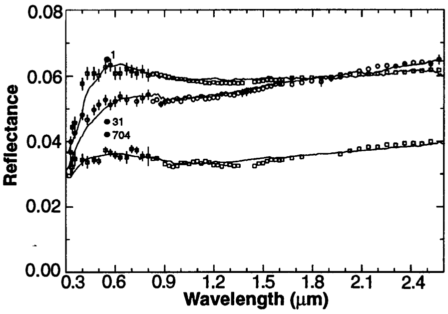

Fig. 2. Close counterparts found between the C asteroids and carbonaceous chondrites in Fig. 1. Asteroid spectra are scaled for the best fits with meteorite spectra: (top trace) 1 Ceres (G) and Y86720; (middle trace) 31 Euphrosyne (C) and B7904; and (bottom trace) 704 Interamnia (F) and Y82162. The IRAS albedos (*6*) of the asteroids are all scaled by 0.65 and plotted as filled circles for comparison. Vertical lines represent the standard deviation.

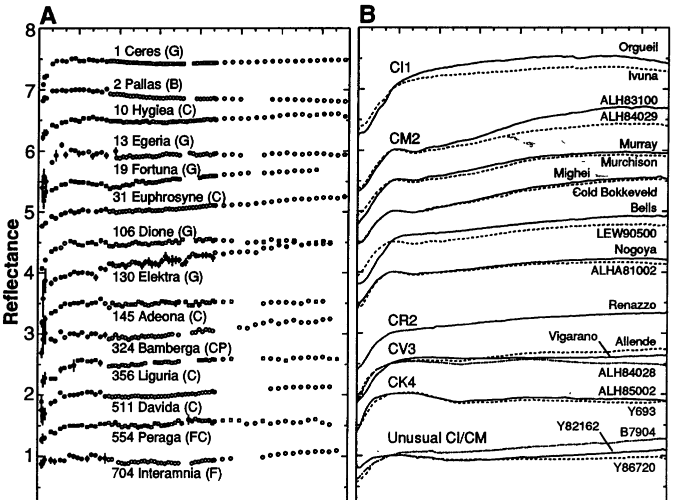

Fig. 1. (**A**) Telescopic reflectance spectra of the C, G, B, and F asteroids (*4*) and (**B**) laboratory reflectance spectra of carbonaceous chondrite powders (<100 or <125 μm) measured at 30° incidence and 0° emergence angles. All reflectance spectra are normalized to 1.0 at a wavelength of 0.55 μm and shifted by 0.5 or 1.0 from each other. Class names of the asteroids are given in parentheses (*1*), and carbonaceous chondrite spectra are grouped according to their subgroups.

T. Hiroi, SN3, NASA Johnson Space Center, Houston, TX 77058.
C. M. Pieters, Department of Geological Sciences, Brown University, Providence, RI 02912.
M. E. Zolensky, SN2, NASA Johnson Space Center, Houston, TX 77058.
M. E. Lipschutz, Department of Chemistry, Purdue University, West Lafayette, IN 47907.

---

*To whom correspondence should be addressed.

atm) hydrogen atmosphere for 1 week at 400°, 500°, 600°, 700°, 800°, 900°, and 1000°C, as a reasonable simulation of the heating processes inside the asteroids made of CM-like materials. Each heated Murchison sample was powdered and sieved into two grain-size fractions (<63 μm and 63 to 125 μm), and their reflectance spectra were measured. We compared the measured reflectance spectra of those heated Murchison samples with averaged reflectance spectra of the five C asteroids and five G asteroids in Fig. 1 (Fig. 3). The UV absorption feature of the average C and G type asteroid spectra is best reproduced by the Murchison sample heated at 600°C and the overall spectral profile at 1000°C. The difference in grain sizes did not significantly affect the UV absorption strength for Murchison powders.

The content of CM2 meteorites is, dominantly, serpentine minerals (including cronstedtite), tochilinite, olivine [mean = 95 mole percent $\mathrm{Mg_2SiO_4}$ ($\mathrm{Fo_{95}}$)], Fe-Ni sulfides, Mg-rich pyroxenes [mean = 98 mole percent $\mathrm{MgSiO_3}$ ($\mathrm{En_{98}}$)], and Fe-Ni metal, with the majority of the anhydrous minerals residing in matrix-supported chondrules and aggregates (8). Profound changes occurred in all of these minerals during the heating experiments of Murchison. By 600°C, the serpentines had begun to dehydrate and recrystallize to olivine and orthopyroxene, which are iron-rich, and tochilinite had largely been converted to troilite. At 800°C, Fe-Ni metal had increased in abundance, at the expense of Fe-Ni sulfides, and coarsened in grain size. At 1000°C, chondrules had begun to recrystallize, and the meteorite consisted dominantly of olivine (mean = $\mathrm{Fo_{80}}$) and pyroxenes (mean = $\mathrm{En_{90}}$) with abundant scattered metal and lesser sulfides. Similar mineralogical changes have occurred in the three unusual CI-CM chondrites, although to a varied and diminished extent (5).

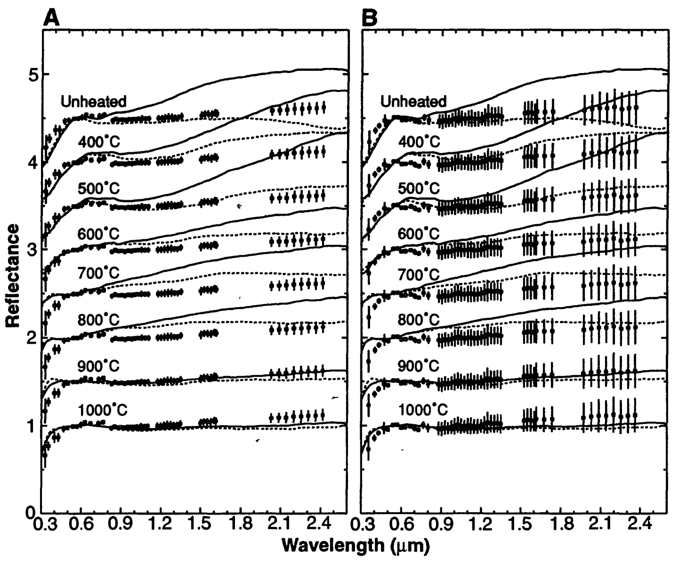

Fig. 3. Reflectance spectra of heated Murchison powders (solid trace, <63 μm; dotted trace, 63 to 125 μm) and the average reflectance spectra of (**A**) the five C asteroids and (**B**) the five G asteroids in Fig. 1. All reflectance spectra are normalized to 1.0 at a wavelength of 0.55 μm and shifted by 0.5 from each other. The standard deviations, of reflectances of five asteroids are shown by vertical bars for the average C and G asteroid spectra.

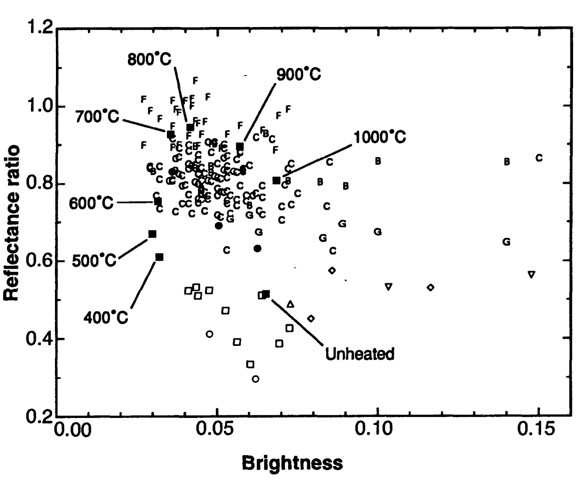

Fig. 4. A plot of the UV-visible reflectance ratio versus visible brightness of 160 C, G, B, and F asteroids and carbonaceous chondrites. The UV-visible reflectance ratio is defined as R(0.337 μm)/R(0.55 μm) of the eight-color asteroid survey (8); the visible brightness is defined by the IRAS albedos for asteroids (6) and R(0.55 μm) for meteorites, where $R(\lambda)$ indicates reflectance at wavelength λ. Class names (C, G, B, and F) are used for the asteroid points; open circles, CI1; open squares, CM2; open triangles, CR2; open diamonds, CV3; inverted open triangles, CK4; closed circles, unusual CI-CM chondrites; closed squares, Murchison.

To compare a larger number of asteroids with carbonaceous chondrites, we compared the eight-band reflectance data (9) and the IRAS albedos (6) of 160 C, G, B, and F asteroids with carbonaceous chondrite spectra. Two parameters were used for comparison: (i) the scaled UV reflectance R(0.337 μm)/R(0.55 μm) and (ii) the IRAS albedo for the asteroids or R(0.55 μm) for the meteorites, where $R(\lambda)$ indicates the reflectance at wavelength λ (Fig. 4). The reflectance ratios of all 160 C, G, B, and F asteroids are larger than 0.6, and those of carbonaceous chondrites are smaller than 0.6 except for the three unusual CI-CM chondrites and the heated samples of Murchison. Murchison heated at 600°, 700°, 800°, 900°, and 1000°C plots in the crowded region of the C, G, B, and F asteroids. Even if the IRAS albedos of the asteroids are scaled by 0.65 for comparison with meteorites (Fig. 2), those thermally metamorphosed meteorites still share the same region with the C, G, B, and F asteroids in Fig. 4.

The UV absorption strengths of meteorites, which this study relies on, have been observed to vary with particle size (2) because phyllosilicates often show a stronger UV absorption when they exist as fine grains (10), as they do in CM2 meteorites (8). Therefore, particle size of the asteroid regolith would be expected to affect the reflectance spectrum. However, smaller grains are believed to exist in asteroidal regoliths, adhering to the surfaces of larger grains and dominating their reflectance spectra. Micrometeorite impacts, for example, could have produced such fine grains without removing them from the asteroid surfaces. The phase angles of reflectance measurements of asteroids are usually smaller than that used to measure the meteorites (30°). Although the difference of the phase angles can affect the spectral shape, including the UV absorption strength, variations were shown to be small for Allende powder between the phase angles of 4° and 30° (11). Phase-angle dependence of the UV absorption strengths of other carbonaceous chondrite powders should also be small and would not significantly affect the asteroid-meteorite comparison (Fig. 4).

Our results suggest that the most abundant carbonaceous chondrites observed as falls do not really represent the surface material of the observed C, G, B, and F asteroids and that less abundant, thermally altered carbonaceous chondrites are quite similar and can be fragments of these asteroids. Previous studies (12, 13) have suggested that the G, B, and F asteroids are thermally metamorphosed objects. The results of this study of unusual CI-CM chondrites and the heated Murchison imply that virtually all the larger C, G, B, and F asteroids are thermally metamorphosed to various degrees. The CK meteorites may be metamorphosed carbonaceous chondrite material, but if so, the metamorphism was of the closed-system variety. Patterns of labile trace elements in three CK chondrites resemble those of 39 other carbonaceous chondrites (*14*) and contrast sharply with those of the three unusual CI-CM chondrites (*5*) and heated Murchison (*7*), determined in an open system. With regard to trace elements and spectral reflectances, no CK metamorphism was identical to that experienced by the large C, G, B, and F asteroids whose spectra have been measured, which suggests that the process of metamorphism varied among the asteroids.

The difference between most carbonaceous chondrites and the C, G, B, and F asteroid surface materials may lie in the fact that all the observed asteroids are large [10 to 1000 km in diameter (*6, 9*)], with a possibly greater opportunity to have been thermally metamorphosed. Friable, unmetamorphosed surface materials similar to most carbonaceous chondrites could have been abraded away by subsequent impact processing, forming smaller asteroids and fragments. The carbonaceous chondrites we now have may derive from a restricted, unrepresentative number of small relatives of the C, G, B, and F asteroids, located at dynamically favorable positions. There has been a similar problem in relating the common S asteroids to the ordinary chondrites, and it has been suggested that the ordinary chondrites are also derived predominantly from small unobserved asteroids (*13*).

Infrared reflectance spectra of CI and CM chondrites usually show strong absorption bands around 3 μm because of hydrated silicates, and the unusual, naturally heated CI-CM chondrites B7904, Y82162, and Y86720 still show a weak absorption band near 2.9 μm (*15*). Similar absorption bands were also observed for many C, G, B, and F asteroids (*16*). Thermal metamorphism of the unusual CI-CM chondrites and these asteroids should have been heterogeneous, preserving some relatively unheated materials. It is also possible that the asteroids were originally formed of anhydrous silicates and water ice and that those silicates subsequently underwent different degrees of aqueous alteration. If the observed 3.1-μm band of 1 Ceres (*16*) is attributable to water ice, Ceres may not have undergone any extensive thermal metamorphism.

REFERENCES AND NOTES

1. Classifications are based on those of D. J. Tholen [in *Asteroids II*, R. P. Binzel, T. Gehrels, M. S. Matthews, Eds. (Univ. of Arizona Press, Tucson, 1989), pp. 1139–1150].
2. T. V. Johnson and F. P. Fanale, *J. Geophys. Res.* **78**, 8507 (1973); F. Vilas and M. J. Gaffey, *Science* **246**, 790 (1989).
3. M. J. Gaffey, *J. Geophys. Res.* **81**, 905 (1976).
4. C. R. Chapman and M. J. Gaffey, in *Asteroids*, T. Gehrels, Ed. (Univ. of Arizona Press, 1979), pp. 1064–1089; J. F. Bell, P. D. Owensby, B. R. Hawke, M. J. Gaffey, *Lunar Planet. Sci.* **19**, 57 (1988).
5. K. Tomeoka, H. Kojima, K. Yanai, *Proc. NIPR Symp. Antarct. Meteorites* **2**, 36 (1989); *ibid.*, p. 55; K. Tomeoka, *ibid.* **3**, 40 (1990); J. Akai, *ibid.*, p. 55; R. L. Paul and M. E. Lipschutz, *ibid.*, p. 80; Y. Ikeda, *ibid.* **5**, 49 (1992).
6. E. F. Tedesco, in *Asteroids II*, R. P. Binzel, T. Gehrels, M. S. Matthews, Eds. (Univ. of Arizona Press, Tucson, 1989), pp. 1090–1138.
7. S. D. Matza and M. E. Lipschutz, *Proc. Lunar Planet. Sci. Conf.* **8**, 161 (1977).
8. M. E. Zolensky and H. Y. McSween, Jr., in *Meteorites and the Early Solar System*, J. F. Kerridge and M. S. Matthews, Eds. (Univ. of Arizona Press, Tucson, 1988), pp. 114–143; M. E. Zolensky, R. Barrett, L. Browning, *Geochim. Cosmochim. Acta*, in press.
9. B. Zellner, D. J. Tholen, E. F. Tedesco, *Icarus* **61**, 355 (1985).
10. T. V. V. King, thesis, University of Hawaii (1986).
11. J. Gradie and J. Veverka, *Proc. Lunar Planet. Sci. B* **12**, 1769 (1981).
12. D. J. Tholen, thesis, University of Arizona (1984).
13. J. F. Bell, D. R. Davis, W. K. Hartmann, M. J. Gaffey, in *Asteroids II*, R. P. Binzel, T. Gehrels, M. S. Matthews, Eds. (Univ. of Arizona Press, Tucson, 1989), pp. 921–945.
14. X. Xiao and M. E. Lipschutz, *J. Geophys. Res.* **97**, 10199 (1992).
15. M. Miyamoto, *Proc. NIPR Symp. Antarct. Meteorites* **5**, 155 (1992).
16. M. A. Feierberg, L. A. Lebofsky, D. J. Tholen, *Icarus* **63**, 183 (1985); T. D. Jones, L. A. Lebofsky, J. S. Lewis, M. S. Marley, *ibid.* **88**, 172 (1990).
17. We thank J. F. Bell for the 52-color asteroid reflectance spectra; M. Miyamoto and H. Y. McSween, Jr., for helpful suggestions; F. Vilas and M. J. Gaffey for the review of the manuscript; the National Institute of Polar Research and the Meteorite Working Group for the loan of antarctic meteorites; Brown University, where reflectance spectra of meteorite powders were measured at RELAB, a multiuser facility operated under National Aeronautics and Space Administration (NASA) grant NAGW-748; and S. Pratt for assistance with the measurements. Supported by NASA grants NAG 9-48 (M.E.L.) and NAGW-28 (C.M.P.) and by the NASA Origins of Solar Systems Program (M.E.Z.). This work was done while T.H. held a National Research Council–NASA/Johnson Space Center Research Associateship.

29 March 1993; accepted 1 July 1993

Surface Tension Measurements of Surface Freezing in Liquid Normal Alkanes

X. Z. Wu, B. M. Ocko, E. B. Sirota, S. K. Sinha, M. Deutsch, B. H. Cao, M. W. Kim

Surface tension measurements reveal surface freezing in liquid *n*-alkanes. A solid monolayer of molecules is found to exist up to 3°C above the bulk freezing point. This surface phase exists only for carbon numbers $14 < n \leq 50$. The measured carbon number and temperature dependence of the surface tension is interpreted within a simple thermodynamical model based on known bulk latent heat data and surface energy considerations. The vanishing of the surface phase for $n \leq 14$ is a possible transition from surface freezing to surface melting behavior.

The role of the free surface in the nucleation of bulk melting or freezing is a subject of much current theoretical (*1–3*) and experimental (*4–10*) interest. As two-dimensional critical temperatures are in general lower than their three-dimensional counterparts, surface melting, where an equilibrium layer of the melt wets the surface of a solid at temperatures below its bulk freezing point T_f, is typical of virtually all solids studied (*1*). It has been observed in a variety of different systems, such as metals (*4*), semiconductors (*5*), inert gas films (*6*), ice (*7*), and most recently, molecular crystals (*8*). By contrast, the opposite phenomenon of surface freezing, where an ordered layer forms at the surface of an isotropic liquid above its bulk freezing point, was observed only in liquid crystals (*9*) and alkanes (*10*). The freezing phenomena in these systems appear to be related: The alkane hydrocarbon chain is a basic component of liquid crystals; however, the liquid crystal surface layers exhibit only liquid-like order (*9*), whereas the order in the alkane surface layer is crystalline (*10*). Surface freezing and melting effects are classified as wetting phenomena, where the system's free energy is lowered when the bulk's surface is wetted by the different surface phase. The thickness of the surface layer at a given temperature is determined by the balance between surface and bulk energies. As the balance is temperature-dependent in general, a system may exhibit either complete wetting, for which the surface layer thickness diverges upon approaching T_f, or partial wetting, for which it remains finite at T_f. To our knowledge, no system exhibiting a transition from surface freezing to melting behavior has been reported.

X. Z. Wu, E. B. Sirota, S. K. Sinha, B. H. Cao, M. W. Kim, Corporate Research Science Laboratory, Exxon Research and Engineering Co., Annandale, NJ 08801.
B. M. Ocko, Physics Department, Brookhaven National Laboratory, Upton, NY 11973.
M. Deutsch, Physics Department, Bar Ilan University, Ramat Gan 52900, Israel.